ASCE

Use of Vertical and Inclined Walls to Mitigate the Interaction of Reverse Faulting and Shallow Foundations: Centrifuge Tests and Numerical Simulation

Alireza Saeedi Azizkandi[1]; Mohammad Hassan Baziar, A.M.ASCE[2]; Sadegh Ghavami, S.M.ASCE[3]; and Sajjad Heidari Hasanaklou[4]

Abstract: This research introduces a new effective approach, including a weak vertical wall (WVW) and a strong inclined wall (SIW) under a shallow foundation, to reduce the rotations caused by a fault rupture. A series of centrifuge tests, followed by numerical modeling and verified by the test results, were conducted to explore the most suitable characteristics of an inclined wall. It is shown that a WVW is, in some cases, ineffective when it is not in the fault rupture path. Furthermore, uncertainties related to determining the exact location of the fault outcrop make it essential to construct a SIW beneath a foundation to protect the foundation that has already been improved by the WVW. The results proved that the application of the proposed approach could reduce the damage potential to the surface and embedded foundations located at various positions relative to reverse faults with various dip angles. **DOI: 10.1061/(ASCE)GT.1943-5606.0002433.** © *2020 American Society of Civil Engineers.*

Author keywords: Fault rupture; Weak vertical wall (WVW); Strong inclined wall (SIW); Numerical analysis; Centrifuge test.

Introduction

Fault is geologically defined as a discontinuity in the geological medium along which relative displacement takes place (Ulusay et al. 2002). This discontinuity may reach the ground surface and cause differential displacement in surface structures. The resultant movement at the ground surface can damage infrastructures by breaking utilities, displacing bridge components, and inducing structural damage in buildings (Oettle and Bray 2013). Observations after the main shocks of recent earthquakes showed satisfactory performance of relatively heavy or stiff structures, supported by continuous and rigid foundations. In some cases, these foundations were able to divert the fault rupture (Faccioli et al. 2008; Bransby et al. 2008; Baziar et al. 2014).

It has been found that foundation systems play a crucial role in the response of structures to emerge dislocations. Structures supported on a rigid mat or box-type foundations performed quite well, in contrast to those on isolated footings or piles. Stiff buildings, founded on rigid box-type foundations, may force fault ruptures to divert (Anastasopoulos and Gazetas 2007a, b). Also, observations after the 1999 Chi-Chi earthquake (Kelson et al. 2001) and 1992 Landers earthquake (Murbach et al. 1999) proved that massive and adequately reinforced concrete slab foundations locally influenced the style and location of near-surface deformations. Two possible main indicators of foundation distress were considered in determining the performance of foundation–structure systems over a rupturing fault: (1) excess foundation rotation, and (2) gap formation beneath the foundation (Ahmed and Bransby 2009; Ashtiani et al. 2016). A gap zone beneath a foundation, where soil loses contact with the foundation, induces stresses and provokes significant bending moments in the foundation. Where ground deformation causes the rigid body rotation of a foundation-structure system, it is important to evaluate system performance acceptability when determining the damage state (Bird et al. 2006). It should be noted that a small initial inclination, caused by differential settlements, for tall structures may initiate toppling collapse much earlier due to leaning instability (Puzrin et al. 2010). For tall structures, Baziar et al. (2019) proposed the following structural damage limits due to foundation rotation (Table 1).

The main geotechnical strategy against dip-slip faulting to protect such structures is focused on diverting fault ruptures away from the foundation and therefore reducing rigid body rotation of the structure. Bray et al. (1993) investigated the effectiveness of soil-reinforcement in spreading localized fault displacement over a wider zone and showed that it minimizes the differential settlement and tensile strains of shallow foundations. Baziar et al. (2014) confirmed that the application of geosynthetic layers in the soil, as a potential mitigation scheme for surface fault rupture hazard, could be effective. Fadaee et al. (2013, 2016) used thick diaphragm-type soil bentonite, installed in front of and near the foundation, to protect a structure founded on a rigid raft. They showed that a weaker and more compressible soil bentonite wall is efficient in diverting the fault rupture and absorbing the imposed faulting–induced

[1]Assistant Professor, School of Civil Engineering, Iran Univ. of Science and Technology, Tehran 13114-16846, Iran (corresponding author). Email: asaeedia@iust.ac.ir

[2]Professor, School of Civil Engineering, Iran Univ. of Science and Technology, Tehran 13114-16846, Iran. Email: baziar@iust.ac.ir

[3]Ph.D. Candidate, School of Civil Engineering, Iran Univ. of Science and Technology, Tehran 13114-16846, Iran. ORCID: https://orcid.org/0000-0001-5102-7658. Email: s_ghavamijamal@civileng.iust.ac.ir

[4]Graduated Student, School of Civil Engineering, Iran Univ. of Science and Technology, Tehran 13114-16846, Iran. Email: sajjad.heidari20@yahoo.com

Note. This manuscript was submitted on September 21, 2019; approved on August 18, 2020; published online on November 18, 2020. Discussion period open until April 18, 2021; separate discussions must be submitted for individual papers. This paper is part of the ***Journal of Geotechnical and Geoenvironmental Engineering***, © ASCE, ISSN 1090-0241.

Table 1. Rotation limits and the corresponding damage levels

Slab rotation	Damage level
$0° \le \theta < 1°$	Slight
$1° \le \theta < 2°$	Moderate
$2° \le \theta < 5°$	Severe
$\theta \ge 5°$	Threatening stability

Source: Data from Baziar et al. (2019).

deformation. Ashtiani et al. (2018) evaluated the effectiveness of a vertical trench adjacent to the foundation filled with three different types of materials including lightweight expanded clay aggregate, a clay mixture composed of kaolinite and water, and expanded polystyrene sheets (EPS). The results indicated that the material with low shear strength and high compressibility (such as EPS) was able to protect the foundation by absorbing fault-induced shear strains in the soil stratum [Fig. 1(a)].

Baziar et al. (2019) indicated that the effectiveness of an expanded polystyrene sheet (EPS) wall depends mainly on the geometry [width (W) and depth (H)] and location of the wall, foundation position (S), fault throw (h), and fault dip angle (α). They mentioned that if the installed wall is not in the fault rupture path, the faulting zone develops toward the foundation, and the resultant excessive rotation of an unprotected foundation can cause significant damages to its building [Fig. 1(b)]. They showed that such foundation rotation is especially the case when a reverse fault dip angle is 60° (for a surface foundation at position $S/B = -0.25$ and an embedded foundation at position $0 \le S/B \le 0.25$) or 75° (for a surface foundation at position $0 \le S/B \le 0.25$ and an embedded foundation at position $0 \le S/B \le 0.5$). Summary of protectable positions for a rigid foundation with EPS wall mitigation based on the rigid body rotation of foundation is displayed in Table 2.

Because there is uncertainty in specifying underground fault traces, any desired weak vertical wall (WVW) distance to the foundation for escaping a fault zone should be based on a lack of reliance. Therefore, the important question remains: what can be done in cases where a WVW is ineffective due to it not being intercepted by the fault rupture path?

This study proposes a solution for mitigating the hazard of a fault rupture for a building protected by the EPS wall when there is no assurance of intercepting the fault trace with the EPS wall. In this regard, trenching an inclined wall beneath the foundation, filled with concrete, seems to be useful in diverting the fault trace. A series of centrifuge tests were conducted to prove the theory and were followed by numerical modeling, verified by the test results, to explore the most suitable characteristics of an inclined wall. It should be noted that the role of an inclined wall is scrutinized in cases where placing a WVW is unable to reduce the hazard of a fault rupture satisfactorily. The final part of this paper numerically evaluates the effect of S/B on foundation position for both surface and shallow embedded foundations. In some cases (for example, $S/B = 0.5$ and 0.75 in fault dip angle = 60°), the vertical wall is effective alone, and the inclined wall has no role in the hazard mitigation. In other cases, where the vertical wall is not effective, the inclined wall can intercept the rupture path, and the foundation is protected by this new method.

Centrifuge Modeling

The faulting tests under 50-g centrifugal acceleration were carried out at the centrifuge facility of the University of Tehran. The split box (Fig. 2), with 75° dip angle reverse faulting was constructed with outer dimensions 100 cm in length, 50 cm in width, and 45 cm in height; and internal dimensions 63 cm in length, 49 cm in width, and 34 cm in height. The bottom of the box was designed to be movable by a hydraulic jack and hence capable of simulating the movements of reverse faulting. The length of the hanging wall was 20 cm, and the maximum allowable offset of the fault with the 75° dip angle was 5 cm (2.5 m in the prototype scale).

A uniformly graded fine clean Firoozkuh sand No. 161 deposit with a relative density of $D_r = 60\%$, moisture content of 5% (corresponding to $\gamma_{wet} = 16.05$ kN/m^3), and thickness of 24 cm (12 m at prototype scale) was poured into the box. The properties of Firoozkuh sand No. 161 are given in Table 3. Peak friction angle $\phi_p = 33°$, residual friction angle $\phi_{res} = 31°$, and peak dilation angle $\Psi_p = 1°$ were measured for $D_r = 60\%$ and a moisture content of 5% (Ashtiani et al. 2016).

In these experiments, 3-cm thick sand layers were poured into the soil box and compacted homogeneously by a calibrated steel hammer. After each soil layer was poured, a thin colored sand layer was placed in close proximity to the Plexiglas side to highlight the rupture path and shear localization from the front face.

Two centrifuge tests with 50-g acceleration were performed for this study. The first test was conducted on the free-field condition to

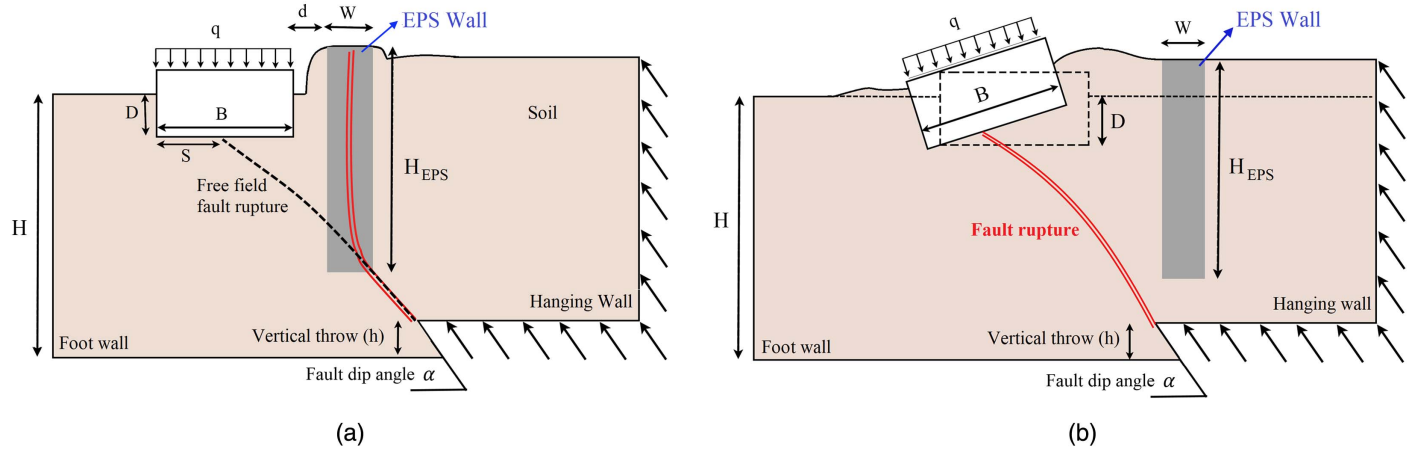

Fig. 1. Effectiveness of expanded polystyrene sheet (EPS) wall: (a) placement of EPS leads to fault rupture diversion and mitigation of the foundation rotation; and (b) EPS wall cannot divert fault rupture path.

J. Geotech. Geoenviron. Eng., 2021, 147(2): 04020155

Table 2. Summary of protectable positions for rigid foundation with EPS wall mitigation based on the rigid body rotation of foundation

Fault dip angle (α) (degrees)	Foundation position (S/B)	Without EPS wall		With EPS wall	
		Surface foundation ($D/B = 0$)	Shallow embedded foundation ($D/B = 0.3$)	Surface foundation ($D/B = 0$)	Shallow embedded foundation ($D/B = 0.3$)
45	1.25	Slight	Slight	Slight	Slight
	1	Slight	Moderate	Slight	Slight
	0.75	Slight	Threatening stability	Slight	Slight
	0.5	Severe	Threatening stability	Moderate	Slight
	0.25	Threatening stability	Threatening stability	Slight	Slight
	0	Threatening stability	Threatening stability	Slight	Moderate
	−0.25	Threatening stability	Severe	Slight	Severe
60	1.25	Slight	Slight	Slight	Slight
	1	Slight	Moderate	Slight	Slight
	0.75	Slight	Threatening stability	Slight	Slight
	0.5	Severe	Threatening stability	Slight	Slight
	0.25	Threatening stability	Threatening stability	Slight	Threatening stability
	0	Threatening stability	Threatening stability	Severe	Threatening stability
	−0.25	Threatening stability	Severe	Threatening stability	Severe
75	1.25	Slight	Slight	Slight	Slight
	1	Slight	Slight	Slight	Slight
	0.75	Slight	Threatening stability	Slight	Moderate
	0.5	Severe	Threatening stability	Slight	Threatening stability
	0.25	Threatening stability	Threatening stability	Threatening stability	Threatening stability
	0	Threatening stability	Threatening stability	Threatening stability	Threatening stability
	−0.25	Severe	Moderate	Severe	Moderate

Source: Data from Baziar et al. (2019).

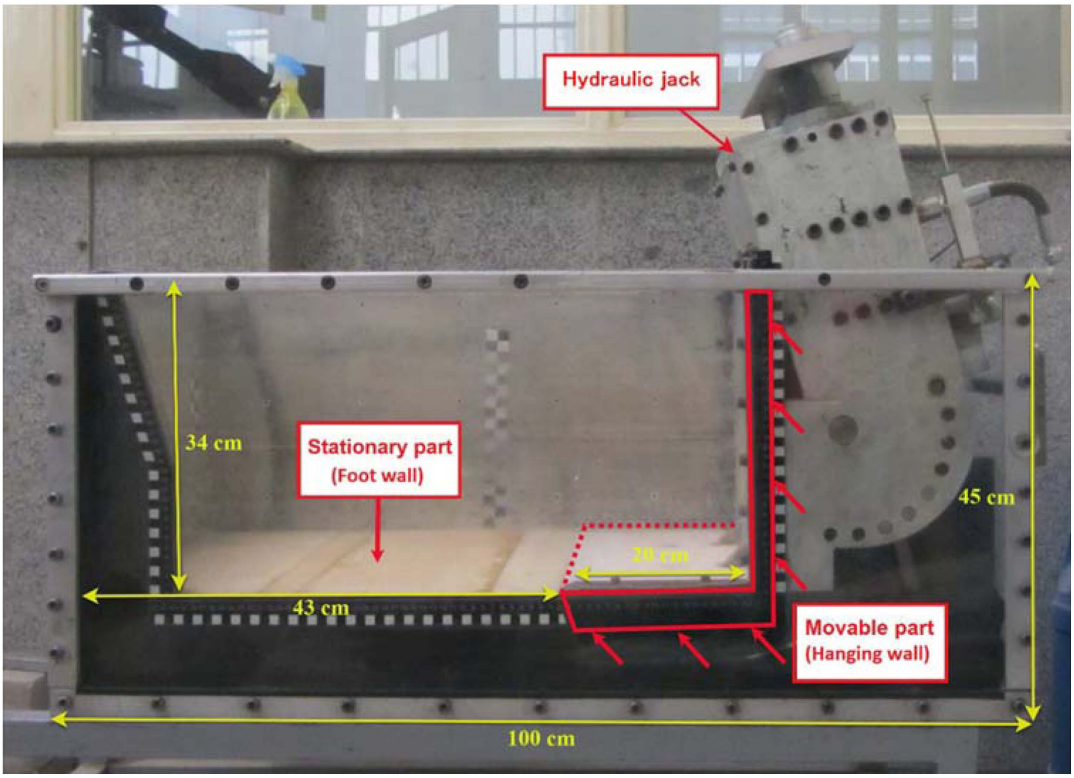

Fig. 2. Split box for modeling fault displacement in geotechnical centrifuge.

determine the fault rupture path as well as to select the position (S) of the foundation, with respect to its emergence. The second test was performed to evaluate the effectiveness of the inclined wall, as a hazard mitigation technique associated with reverse faulting, to protect the shallow foundation from the fault rupture.

For modeling the inclined wall, the soil layers were first compacted in a manner similar to the model when the nonmitigated scenario was considered. Then, a part of the filled sand layers was excavated to reach the desired location planned for the rigid inclined wall with an angle of $\beta = 36°$ (with horizontal axis).

Table 3. Summary of soil properties used for experiments

Name	D_{50}	e_{max}	e_{min}	G_s
Firoozkuh sand number 161	0.3 mm	0.943	0.603	2.658

Source: Data from Moghadam et al. (2009).

In order to design reduced-scale models of piles, walls, and tunnels similar to the prototype, it is important to make their bending stiffness (EI) equal using the following equation:

$$E_m I_m \times N^4 = E_p I_p \quad (1)$$

where N = gravity level in the centrifuge test; E_m = Young's modulus of the model; E_p = Young's modulus of the prototype; I_m = cross-sectional moment of inertia of the model; and I_p = cross-sectional moment of inertia of the prototype. Based on Eq. (1), an aluminium plate of 300 mm × 4 mm (length and thickness in the model) combined with Young's modulus of 70 GPa was used to simulate a concrete inclined slab wall of 15 × 0.56 m (length and thickness in prototype) with Young's modulus of 25 GPa. In other words, model sections may be typically made from different polymeric materials or aluminum (Hayward et al. 2000; Abdoun et al. 2003; Knappett and Madabhushi 2009; Azizkandi et al. 2019; Baziar et al. 2020) to simulate the prototype concrete material. Choo et al. (2010) and Zeping et al. (2014) also used an aluminum plate to properly model the bending stiffness of the prototype concrete face in the concrete faced rock-fill dam.

A rigid steel with a breadth of $B = 170$ mm (8.5 m at prototype scale) and thickness of $t = 21$ mm was installed at the $S/B = 0$ position to model a rigid shallow foundation in the centrifuge test. This foundation can bear a pressure of $q = 81$ kPa, representing an 8-story building with a minimum value of 10 kPa per story (Fig. 3).

To monitor the movement and rotation of the foundation during testing, three linear variable displacement transducers (LVDTs), as indicated in Fig. 3, were installed. Another LVDT was also set on the hydraulic jack to monitor the progress of the fault offset. Measurement of soil deformation was achieved using particle image velocimetry (PIV), and then the GeoPIV software was used to analyze the digital images of the soil sample (White et al. 2003).

Finite-Element Modeling and Validation

The ABAQUS (2014) software, as based on the finite-element approach, was utilized for conducting the numerical analysis. The prototype dimensions of the test under two-dimensional (2D) plane strain conditions were chosen for numerical modeling.

The soil body was modeled with structured quadrilateral continuum finite elements. After experimenting with several mesh models, the best mesh dimensions in terms of accuracy and runtime were selected. The choice of a very refined mesh (measuring 1m or less) in the probable region of the soil rupture is a prerequisite for a successful numerical simulation (Gazetas et al. 2008). Therefore, an area of 0.5 × 0.5 m was selected for the probable fault rupture region in the soil stratum, and the mesh sizes were larger at the soil boundaries. The numerical analysis was conducted in two steps. First, gravity loading was applied to the model. The discontinuity between two parts of the soil was applied to simulate the fault movement. Then, the hanging wall side was moved at the dip angle of 75°, while the foot-wall side of the soil remained stationary as fixed boundary conditions were applied. The vertical boundaries were free to move in a vertical direction when the horizontal boundaries were completely fixed. Fig. 4 shows the finite-element meshing and boundary conditions used in numerical modeling. The tested soil was relatively loose sand, and the Mohr-Coulomb failure criterion was adapted as a constitutive model for the soil stratum. The same soil properties, like those used in the centrifuge modeling, were selected for the numerical analysis.

The foundation with an $S/B = 0$ position was modeled as linear elastic media with high rigidity (Steel). The inclined wall was assumed to be linear elastic with a typical density and stiffness of concrete. The meshing of the wall was modeled using 0.5 m × 0.5 m structural quad elements, as shown in Fig. 4. The interface between soil and foundation was defined by contact type interaction. Using hard contact for normal behavior, the friction coefficient of μ was employed for tangential behavior. To allow for the possibility of separation at the level of contact between the soil and other structures [strong inclined wall (SIW) or foundation), gap element specifications were introduced to the model. Such elements, rigid in compression but tensionless, allow detachment of the foundation or wall from the soil. Properties of the materials used in the foundation and wall in the numerical simulation are summarized in Table 4.

The capability of the numerical analysis in predicting the fault rupture path pattern and the surface displacement was first evaluated in free field condition. Figs. 5(a and c) compare the numerical modeling and the experimental results at $h = 48$ mm offset (2.4-m dislocation at the prototype scale). The rupture path in the experimental result is almost located in the same shear zone as predicted by the numerical modeling, proving the accuracy of the numerical

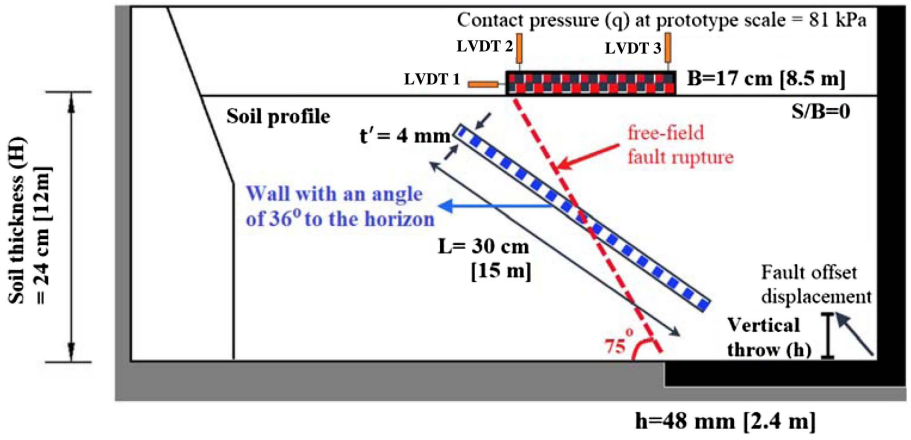

Fig. 3. Schematic configuration of the problem and its geometry in the presented study (brackets = prototype dimensions).

J. Geotech. Geoenviron. Eng., 2021, 147(2): 04020155

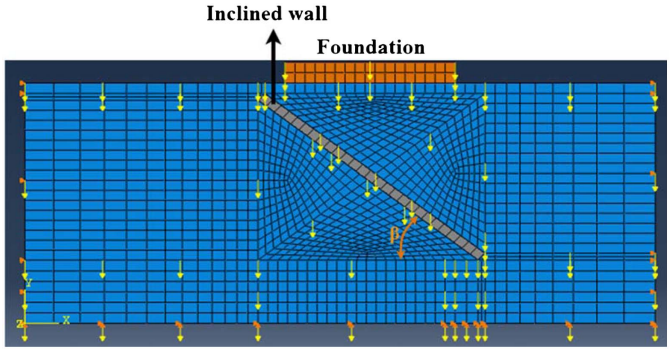

Fig. 4. Two-dimensional finite-element meshes used in the numerical analysis.

Table 4. Properties of the material adopted in the numerical modeling

Material	Unit weight (kN/m^3)	Elastic modulus (GPa)	Poisson's ratio	Friction coefficient, μ
Steel	77.142	200	0.35	0.35
Concrete	24	25	0.28	0.4
EPS	0.117	0.0033	0.07	0.6

analysis. The vertical displacement on the ground surface, driven from the centrifuge test and numerical prediction, are presented in Fig. 6. As can be seen, the numerical model is in good agreement with the experimental results.

Figs. 5(b and d) illustrate the interaction of a 75° reverse fault with the shallow foundation as well as the inclined wall performance in deviating the fault rupture path. Prediction of the numerical analysis on the fault rupture path is in good agreement with the observed rupture path of the centrifuge model. The inclined wall forced the fault rupture to propagate along the wall and hence deviated the rupture path toward the outside of the foundation. As a result, the wall limits the maximum force and strain applied from the ground to the foundation base. If the fault rupture emerges beneath the foundation, it will induce more stress on the foundation. The fault displacement creates a separation between the soil and inclined wall due to its relatively rigid behavior, which is observed in both the physical and numerical models (Fig. 5). The gap zone beneath the wall induces extra stress to the wall (caused by bending moment), which is confirmed by the numerical analysis and shown in Fig. 7. In other words, in practical applications, such bending moments should be considered in the structural design of the wall. The amount of foundation rotation (0.95° in the experimental model) was affected by the inclined wall (Fig. 8), which proves the effectiveness of the wall. As shown in Table 2, the damage level for fault dip angles of 75° and surface foundation at $S/B = 0$ is at the stability threatening stage ($\theta \geq 5°$) for both conditions of with and without an EPS wall. The inclined wall reduced the foundation rotation and caused it to experience a slight level of damage. Fig. 8 shows similar experimental and numerical results for the foundation rotation.

Having validated the numerical modeling, further studies were conducted to investigate cases in which a weak vertical wall fails to intercept the fault rupture (Fig. 1) and also to optimize the characteristics of the inclined wall. An EPS wall ($W = 0.5$ m and $H_{EPS} = 8.5$ m) as a WVW was modeled next to the foundation and constructed from linear elastic–plastic material with 17-kPa yield strength. Baziar et al. (2019) showed that the effectiveness of the WVW depends mainly on the foundation location, embedment depth of the foundation, and fault dip angle and depth. Therefore, a numerical analysis was carried out to find the optimum features for the proposed inclined wall. Then, the effectiveness of utilizing both the EPS vertical wall and the inclined wall with the appropriate material, as a protective method of improving the foundation, was numerically investigated.

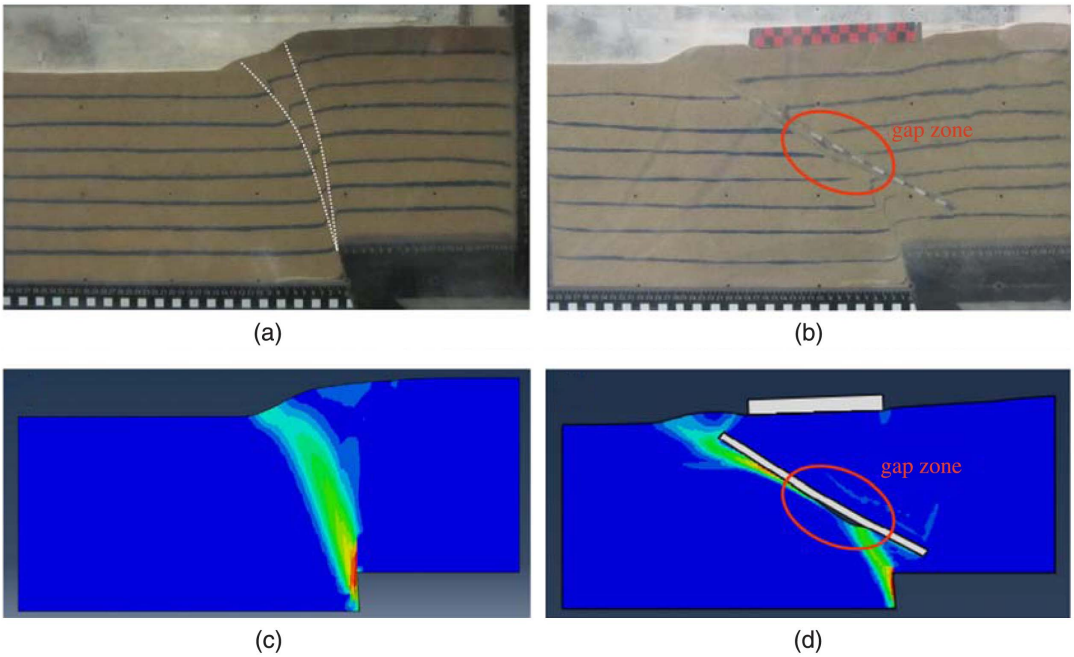

Fig. 5. Comparison between the numerical analysis and centrifuge tests results: (a) centrifuge model for the free field condition; (b) centrifuge model for the test with foundation, positioned at $S/B = 0$ and inclined wall; (c) deformed mesh with plain strain contours for the free-field condition in the numerical analysis; and (d) deformed mesh of numerical analysis for foundation, positioned at $S/B = 0$, and inclined wall.

J. Geotech. Geoenviron. Eng., 2021, 147(2): 04020155

Effect of the Material

Three types of material, namely clay, EPS, and concrete with 20, 3.3, and 25-GPa elastic modulus, respectively, were considered for the inclined wall with $\beta = 36°$ slope and 0.5-m thickness (Fig. 9). As seen in Fig. 9, while EPS walls perform better than clay walls, the foundation rotation is large and the stability of foundation is still threatened. A concrete high shear wall was used, which diverted the fault rupture out of its path and kept the foundation intact. In other words, compared with the other two materials, the least foundation rotation was observed for the inclined wall made of concrete, which proves the effectiveness of using a strong rigid wall. From now on, this wall is called the SIW. The term strong in this case stands for concrete as opposed to the weak vertical wall. The inclined wall must be strong such that it prevents the fault rupture from passing through and reaching the foundation. It should be noted that using the terms "strong wall" addresses the wall's high shear strength in relation with the surrounding soil, whereas the term "weak vertical wall" implies that the constructed wall has a lower shear strength than the surrounding soil, similar to EPSs. The use of SIW reduced the damage level from most dangerous to moderate ($\theta < 2°$) (Baziar et al. 2019).

Effect of Inclination

Five different inclination values ($\beta = 10°$, 20°, 30°, 36°, and 40°) were analyzed to find the optimum slope for the wall. Fig. 10 shows that smaller slope values enable the fault rupture to pass through a major part of the alluvium layer and head toward the foundation. While increasing the slope values enables the path to continue its way up to the left side of the inclined wall, located beneath the foundation, it nevertheless reduces the damage level. It is also seen that the increase in the wall slope leads to better performance, such that an inclined concrete wall with an inclination of $36° < \beta < 40°$ can successfully reduce the damage level to slightly damaged. Damage reduction in such cases is often due to the fact that rupture path diversions occur in deeper depths. As seen in Figs. 10(d and e), the presence of a trenched inclined concrete wall causes the rupture path to deviate and extend along the wall, which prevents the foundation from experiencing excess deformation and rotation. It should be noted that the value of $\beta = 36°$ is only valid for the studied case in the present research.

Effect of Thickness

Similar to wall inclination, four different SIW thicknesses ($t' = 0.5$, 0.75, 1, and 1.5 m) were studied. A thickness of 0.5 m was found to be the optimal thickness for the concrete inclined wall employed in this study. In other words, increasing the wall thickness (up to 0.5 m) decreases the foundation rotation, while increasing the wall thickness beyond 0.5 m increases the foundation rotation.

As seen in Fig. 11, increasing the wall thickness beyond this value reduces the efficiency of the wall and forces the foundation

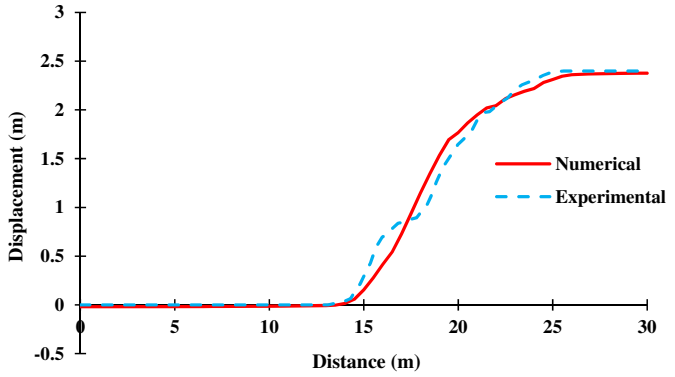

Fig. 6. Vertical displacement of the surface when the fault throw is 2.4 m.

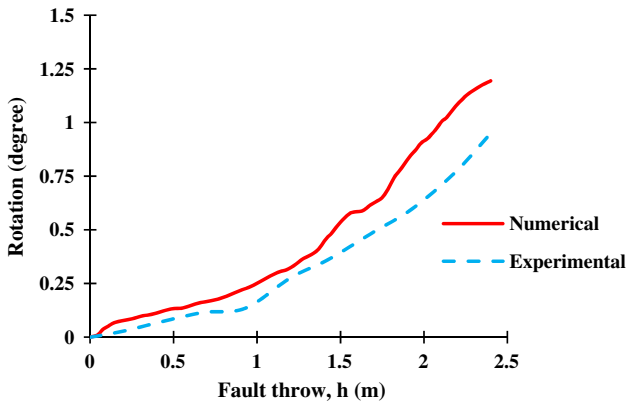

Fig. 8. Foundation rotation versus vertical throw of the fault.

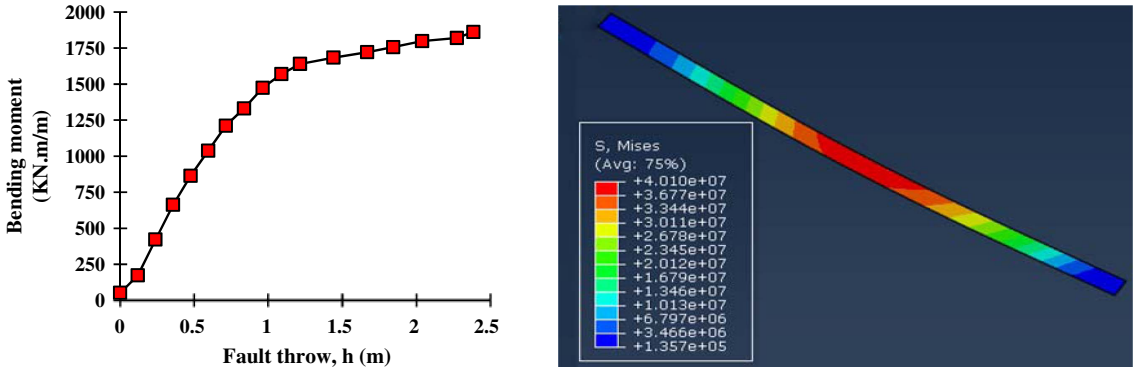

(a) (b)

Fig. 7. (a) Bending moment on middle of the inclined wall against vertical throw of fault in numerical modeling; and (b) stress contours of the inclined wall after faulting.

J. Geotech. Geoenviron. Eng., 2021, 147(2): 04020155

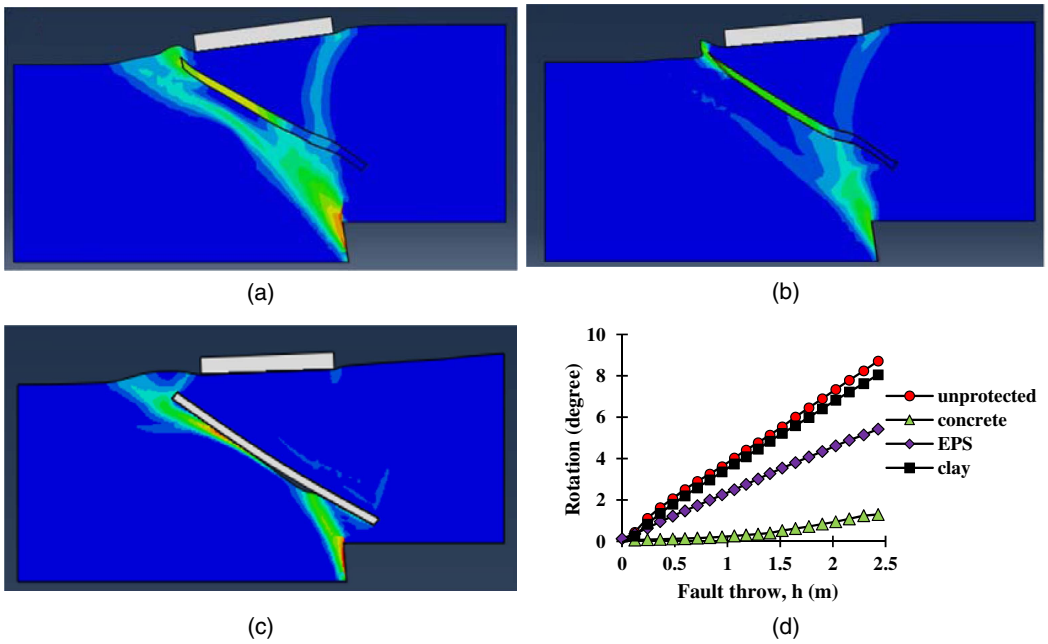

Fig. 9. Effect of using an inclined wall made of three different materials in addition of weak vertical wall: (a) clay; (b) EPS; (c) concrete; and (d) values of foundation rotation.

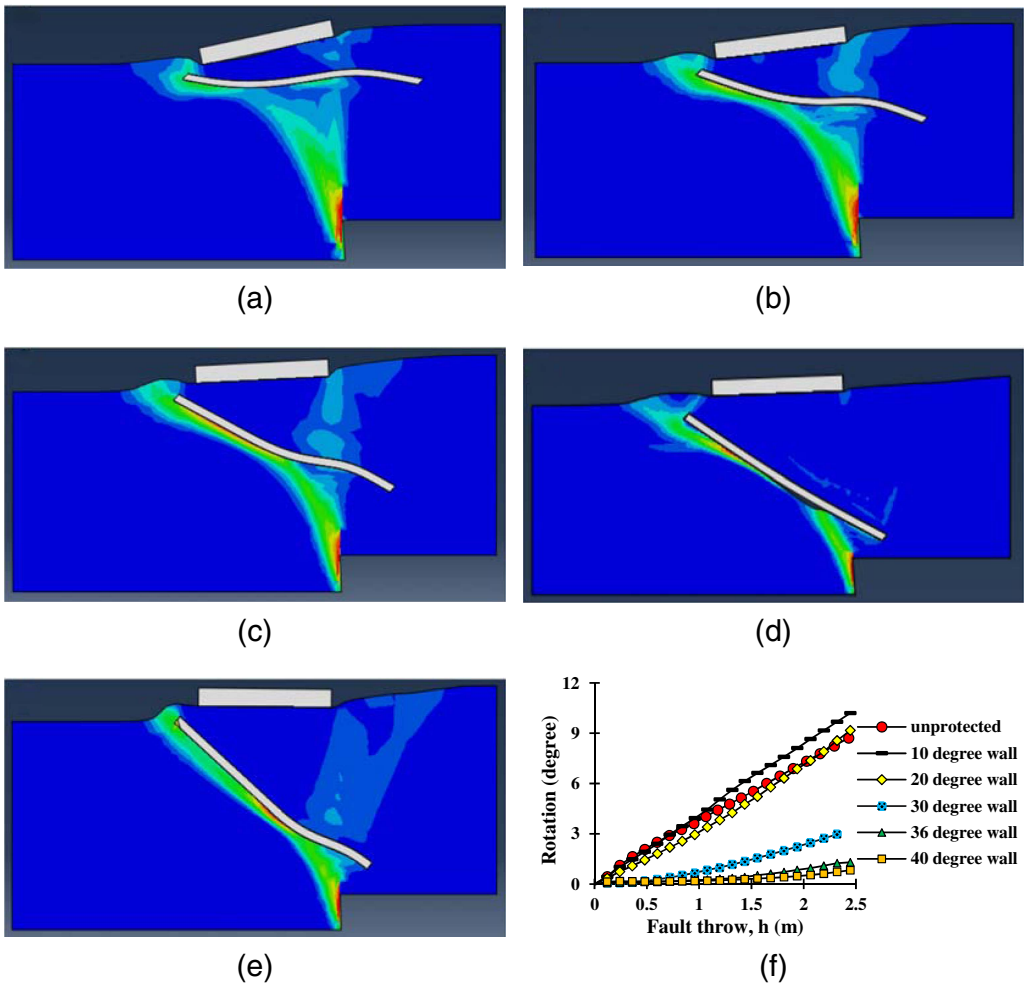

Fig. 10. Inclination effect: (a) $\beta = 10°$; (b) $\beta = 20°$; (c) $\beta = 30°$; (d) $\beta = 36°$; (e) $\beta = 40°$; and (f) values of foundation rotation.

to experience a rigid body rotation. As shown in Figs. 11(b–d), compared with Fig. 11(a), increasing the wall thickness leads to creating another rupture path toward the right side of the wall; consequently, the upward movement of the threw path is transmitted to the right sight of the foundation through the surrounding soil, causing excess rotation in the slab. It should be noted that the optimal wall thickness depends on several factors such as surrounding soil properties, fault rupture path, displacement, and overburden pressure. It is, therefore, crucial that the designed wall has enough rigidity (in terms of the elastic modulus), but not too much, to protect the foundation.

Effect of Foundation Position

The effect of placing a SIW beneath a shallow foundation [at different positions (S/B)], with the presence of an EPS wall in its vicinity, on the interaction of foundation with reverse fault rupture was investigated.

Surface Foundations ($D/B = 0$)

Figs. 12(a and b) show the rotation values for both protected and unprotected surface foundations ($D/B = 0$) placed at various positions and with a reverse fault dip angle of 75°. As can be seen, increasing the fault vertical displacement (h/H) from 8% to 20% induces great rotations in the foundation of all unprotected foundations. As seen for a 75° fault dip angle, the worst case occurs at $S/B = 0.25$, where the surface foundation experiences the greatest rotation. Trenching WVW reduces the damage level at $S/B \geq 0.5$ and $S/B = 0.25$ for small fault displacements [Fig. 12(a)]. In other words, using the WVW reduces the foundation rotation by 50%, whereas no effect was observed for higher displacement values [Fig. 12(b)] at $S/B \leq 0.25$. Figs. 12(a and b) illustrate that the generated protective wedge (SIW, WVW, and foundation) reduces the damage level down to the lowest possible value for all cases. A 50% reduction is observed in the foundation rotation at $S/B = -0.25$ and for $h/H = 20\%$ [Fig. 12(b)], which, in effect, decreases the damage level from stability threatening to moderate. Figs. 12(c and d) show the effectiveness of the proposed protective wedge in reducing the foundation rotation at $S/B = 0.25$ (the worst case of an unprotected foundation).

Figs. 13(a and b) illustrate that reducing the fault dip angle to 60° increases the effectiveness of WVW and enables the foundation to endure lower rotations. The worst foundation location for this state is at $S/B = 0$. Using WVW with predefined features at $S/B \geq 0.25$ reduces the damage level from severe and stability threatening

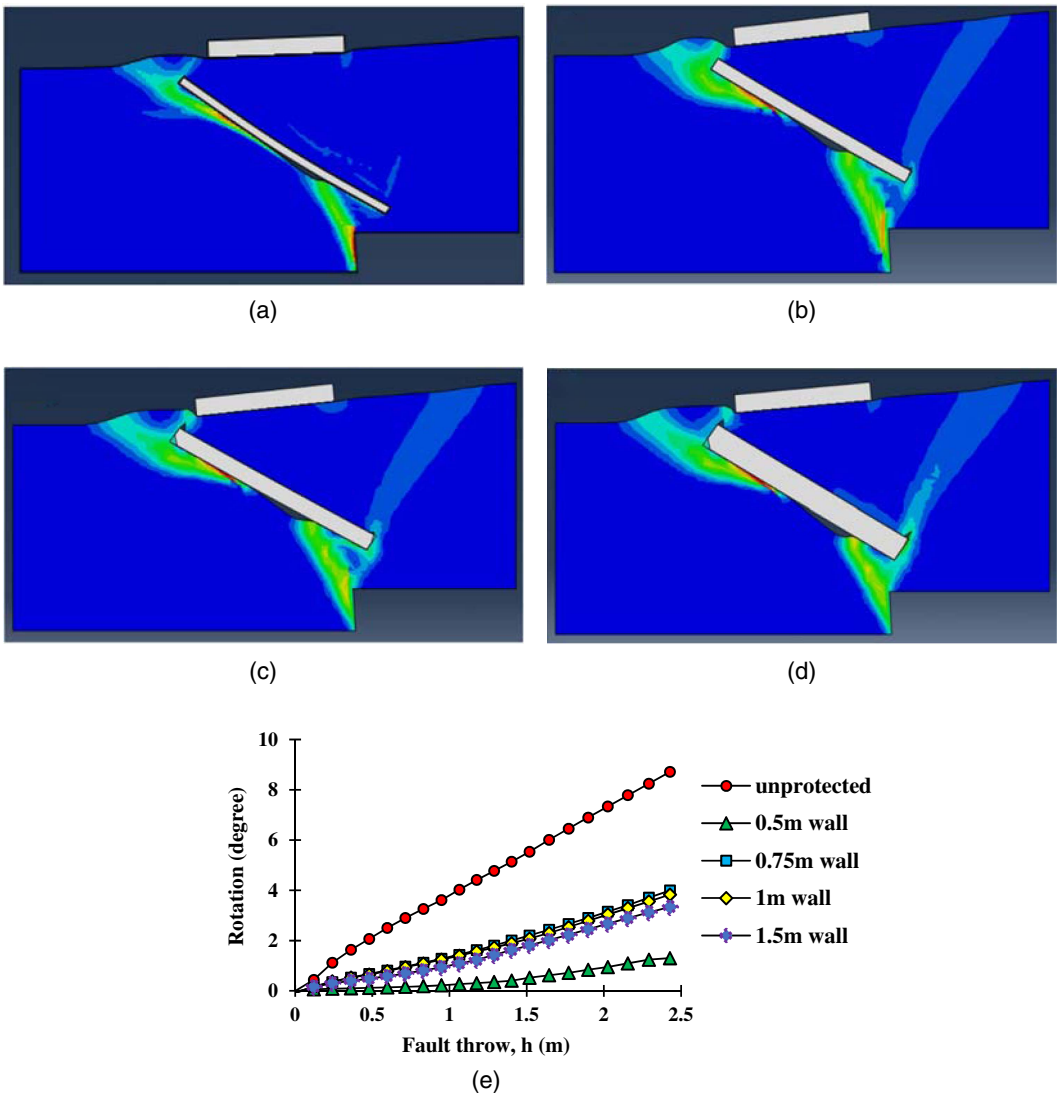

Fig. 11. Inclined wall thickness effect: (a) 0.5 m; (b) 0.75 m; (c) 1 m; (d) 1.5 m; and (e) amounts of foundation rotation.

J. Geotech. Geoenviron. Eng., 2021, 147(2): 04020155

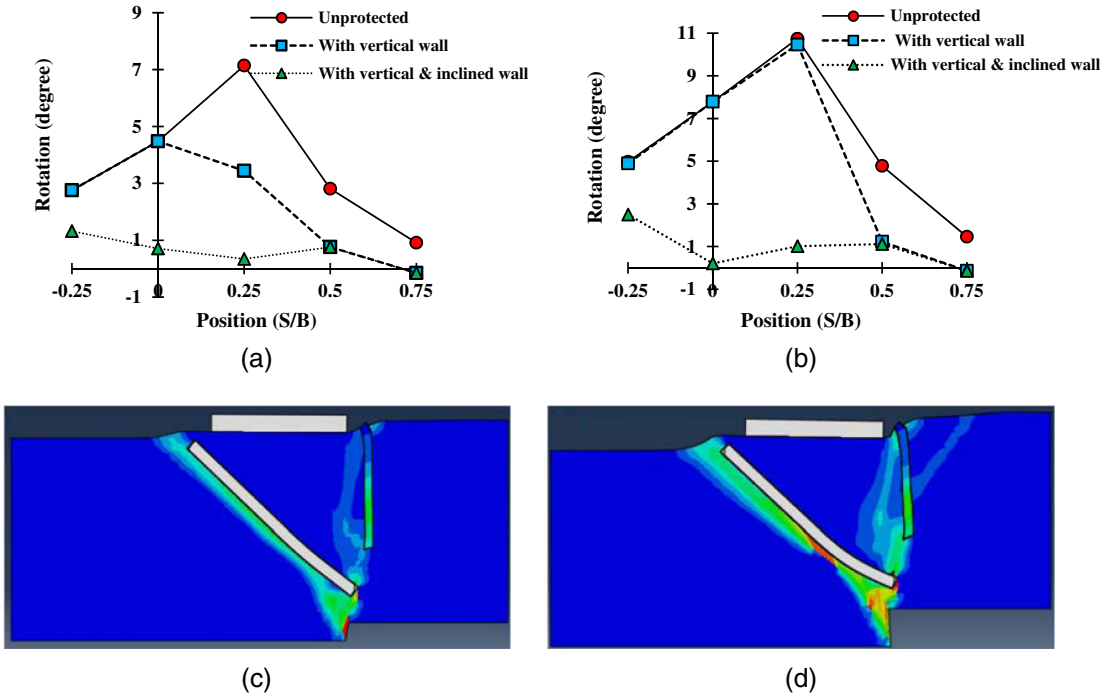

Fig. 12. Effectiveness of using both WVW and SIW to protect a surface foundation ($D/B = 0$) positioned at different locations for fault dip angle of 75°: (a) $h/H = 8\%$; (b) $h/H = 20\%$; (c) finite-element deformed mesh with plastic strain contours for $S/B = 0.25$, $h/H = 8\%$; and (d) finite-element deformed mesh with computed plastic strain contours for $S/B = 0.25$, $h/H = 20\%$.

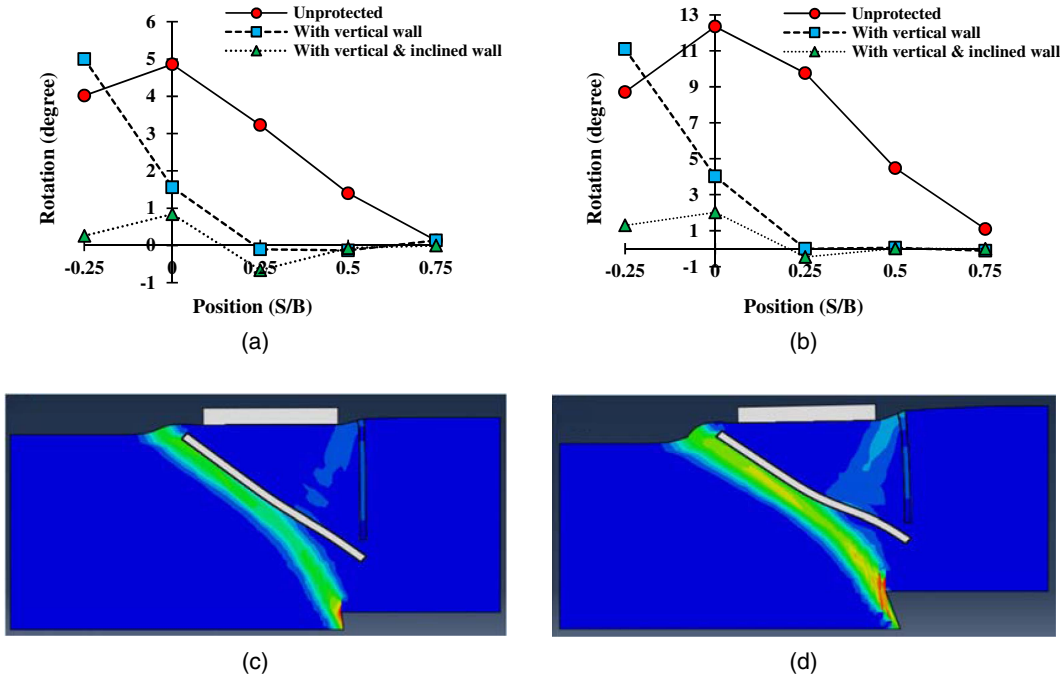

Fig. 13. Effectiveness of using both WVW and SIW to protect a surface foundation ($D/B = 0$) positioned at different locations for fault dip angle of 60°: (a) $h/H = 8\%$; (b) $h/H = 20\%$; (c) finite-element deformed mesh with plastic strain contours for $S/B = -0.25$, $h/H = 8\%$; and (d) finite-element deformed mesh with computed plastic strain contours for $S/B = -0.25$, $h/H = 20\%$.

($2° \le \theta < 5°$, $\theta \ge 5°$) to slight ($\theta < 1°$). As seen in Figs. 13(a and b), placing the foundation closer to the hanging wall reduces the effectiveness of the wall. While a 65% reduction in the foundation rotation is achieved at $S/B = 0$ and for $h/H = 20\%$, the damage level is still severe, and the trenched vertical wall for the case with $S/B = -0.25$ shows to be completely ineffective. The effectiveness of utilizing SIW besides WVW is highlighted at positions $S/B = -0.25$ and 0. Similarly, as displayed in Figs. 13(a and b), the generated protective wedge reduces the damage level down to the lowest possible value for all cases, especially for $S/B = -0.25$,

where it completely protects the foundation and reduces the rotation to less than 1 degree. At $S/B = 0$, the proposed wedge for the lower fault displacement values ($h/H = 8\%$) reduces the damage level down to the slight state, while an 80% reduction in the rotation is observed for the higher values ($h/H = 20\%$). The numerical results of fault rupture diversion for the case with two fault displacement ratios of $h/H = 8\%$ and $h/H = 20\%$ are displayed in Figs. 13(c and d). A protection report for the surface foundation, placed at different positions (S/B) relative to the free-field fault rupture emergence, is summarized in Table 5.

Shallow Embedded Foundation ($D/B = 0.3$)

Figs. 14(a and b) display the effectiveness of using WVW and SIW to protect a shallow embedded foundation with $D/B = 0.3$, placed at different positions, for a 75° dip angle fault. The most critical position for an unprotected foundation and two vertical displacement ratios occurs at $0.25 \le S/B \le 0.5$, where the rotation value is the highest. The use of a trenched WVW shows to have very little effect in this case, such that at $S/B = 0.5$ and a smaller fault displacement ratio ($h/H = 8\%$), in spite of a 50% reduction, only 3 degrees of the rotation caused the foundation to experience severe damage. Increasing the displacement ratio to $h/H = 20\%$ worsens the situation. Similarly, the stability of unprotected cases is still threatened ($\theta \ge 5°$). Using a WVW for the foundation at $S/B = 0.75$ reduces the damage level to slight. Foundations positioned at $S/B < 0.5$ shows that while a trenched vertical wall alone cannot reduce the damage, an inclined wall can successfully protect the foundation and reduce the damage levels. According to Fig. 14(a), for the cases with $h/H = 8\%$, the installed wedge is able to reduce rotation by more than 80% at all foundation positions, and the foundations experience only slight levels of damage ($\theta < 1°$).

Table 5. Summary of protectable positions (S/B) for surface foundation ($D/B = 0$) based on the rigid body rotation of foundation

Fault dip angle (α)	Case	$S/B = -0.25$	$S/B = 0$	$S/B = 0.25$	$S/B = 0.5$	$S/B = 0.75$	$S/B = 1$	$S/B = 1.25$
60°	Unprotected	Threatening stability	Threatening stability	Threatening stability	Severe	Slight	Slight	Slight
	Vertical wall	Threatening stability	Severe	Slight	Slight	Slight	Slight	Slight
	Vertical and inclined wall	Slight	Moderate	Slight	Slight	Slight	Slight	Slight
75°	Unprotected	Severe	Threatening stability	Threatening stability	Severe	Slight	Slight	Slight
	Vertical wall	Severe	Threatening stability	Threatening stability	Slight	Slight	Slight	Slight
	Vertical and inclined wall	Moderate	Slight	Slight	Slight	Slight	Slight	Slight

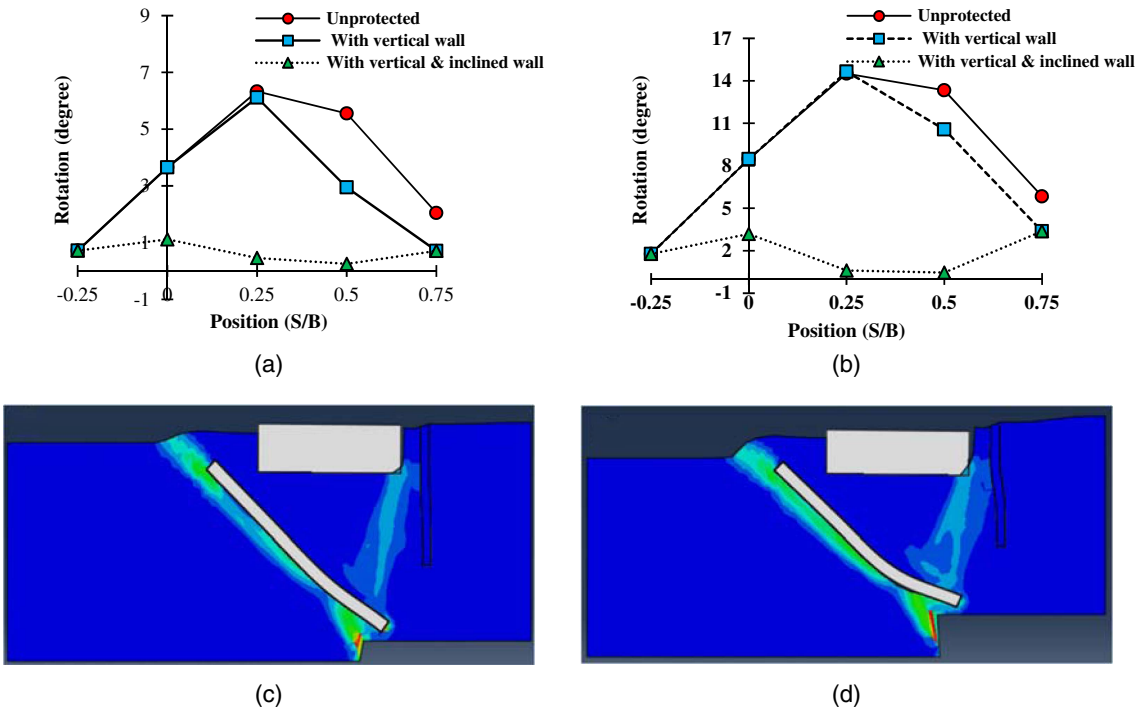

Fig. 14. Effectiveness of using both WVW and SIW to protect a surface foundation ($D/B = 0.3$) positioned at different locations for fault dip angle of 75°: (a) $h/H = 8\%$; (b) $h/H = 20\%$; (c) finite-element deformed mesh with plastic strain contours for $S/B = 0.25$, $h/H = 8\%$; and (d) finite-element deformed mesh with computed plastic strain contours for $S/B = 0.25$, $h/H = 20\%$.

J. Geotech. Geoenviron. Eng., 2021, 147(2): 04020155

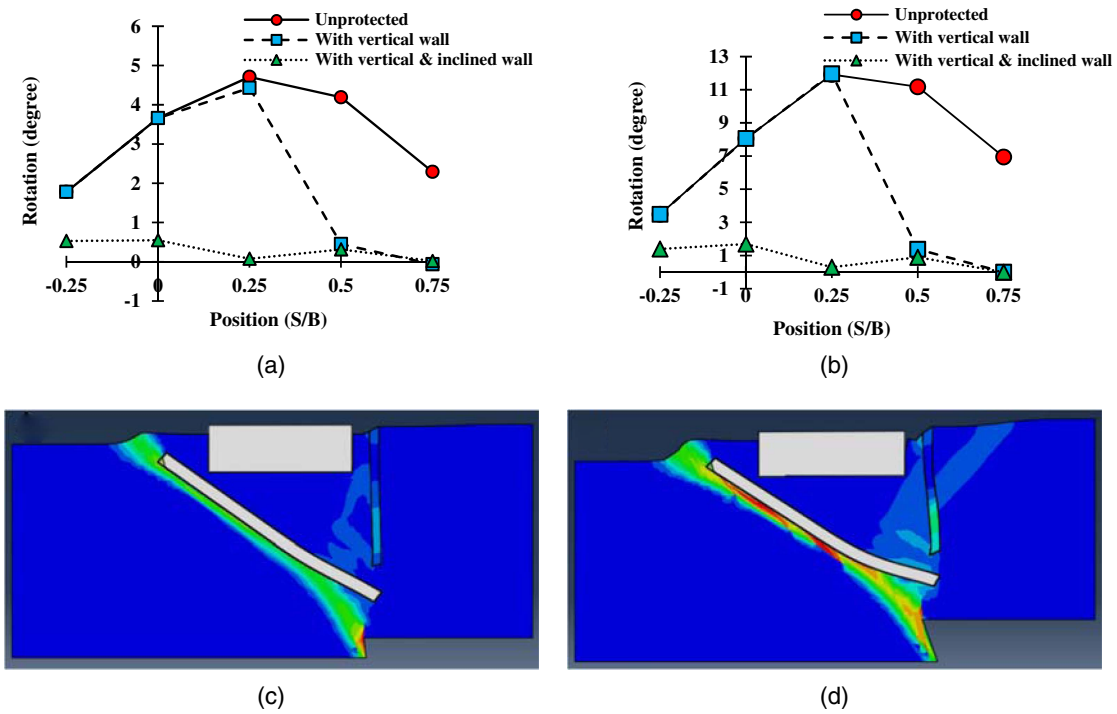

Fig. 15. Effectiveness of using both WVW and SIW to protect a surface foundation ($D/B = 0.3$) positioned at different locations for fault dip angle of 60°: (a) $h/H = 8\%$; (b) $h/H = 20\%$; (c) finite-element deformed mesh with plastic strain contours for $S/B = 0.25$, $h/H = 8\%$; and (d) finite-element deformed mesh with computed plastic strain contours for $S/B = 0.25$, $h/H = 20\%$.

Table 6. Summary of protectable positions (S/B) for shallow embedded foundation ($D/B = 0.3$) based on the rigid body rotation of foundation

Fault dip angle (α)	Case	$S/B = -0.25$	$S/B = 0$	$S/B = 0.25$	$S/B = 0.5$	$S/B = 0.75$	$S/B = 1$	$S/B = 1.25$
60°	Unprotected	Severe	Threatening stability	Threatening stability	Threatening stability	Threatening stability	Moderate	Slight
	Vertical wall	Severe	Threatening stability	Threatening stability	Slight	Slight	Slight	Slight
	Vertical and inclined wall	Moderate	Moderate	Slight	Slight	Slight	Slight	Slight
75°	Unprotected	Moderate	Threatening stability	Threatening stability	Threatening stability	Threatening stability	Slight	Slight
	Vertical wall	Moderate	Threatening stability	Threatening stability	Threatening stability	Moderate	Slight	Slight
	Vertical and inclined wall	Slight	Moderate	Slight	Slight	Moderate	Slight	Slight

Figs. 14(c and d) indicate how a SIW is able to deviate the fault rupture path and protect the embedded foundation, positioned at $S/B = 0.25$ (as the worst case of unprotected foundation).

A fault with a 60-degree dip angle and two vertical displacement ratios ($h/H = 8\%$, 20%, Fig. 15) exhibits the same critical positions ($0.25 \le S/B \le 0.5$) for the highest foundation rotation values. Figs. 15(a and b) display that the use of a WVW decreases the rotation and damage level down to the slight level ($0° \le \theta < 1°$) at $S/B \ge 0.5$. Nevertheless, the trenched vertical wall does not affect the fault displacement ratios, and the rotation values remain the same at $S/B < 0.5$. The use of a SIW, at the same foundation positions, reduces the foundation rotations and the damage level down to the slight state. A rotation reduction of near 100% at $S/B = 0.25$ is greatly noticeable for the case, which shows to have the highest rotation value in the unprotected case. The numerical results, displayed in Figs. 15(c and d), prove the effectiveness of using a SIW for a foundation positioned at $S/B = 0.25$.

A protection report for shallow embedded foundations with $D/B = 0.3$, placed at different positions (S/B) relative to the free-field fault rupture emergence, is summarized in Table 6. As seen in Tables 5 and 6, a trenching WVW is unable to protect a foundation for all cases, and in some situations, it has absolutely no effect on the damage level. The use of a SIW and the created protective wedge as a solution ensures the safety of the foundation. In other words, it can be said that this proposed mitigation scheme, which covers the weak points of using a WVW, is a reliable solution.

Conclusion

The main geotechnical strategy against a dip-slip faulting to protect such structures is focused on diverting fault ruptures away from the foundation, thereby reducing the rigid body rotation of a structure. Installing a WVW with suitable depth and width next

J. Geotech. Geoenviron. Eng., 2021, 147(2): 04020155

to a foundation can deviate the fault rupture path and mitigate the damage level if it is located in the fault rupture path. Cases whereby the rupture moves toward the foundation without being intercepted by such trenched walls question the effectiveness of the WVW.

This research proposed a mitigation scheme, the SIW, to protect shallow foundations from fault-induced damages. The effectiveness of this method is at its peak when coupled with the presence of a WVW. A series of centrifuge model tests and numerical modeling were conducted, and the results confirmed that the presence of a SIW forces the fault rupture to propagate along the wall. In other words, SIW reduced the foundation rotation, which, in effect, reduced the level of structural damage to acceptable values. However, this wall is limited to the maximum force and strain applied from the ground to the foundation.

Placement of a SIW beneath a foundation in addition to a WVW can efficiently absorb and deviate the fault rupture path for cases, in which the WVW fails to intercept the fault rupture alone. Creation of a protective wedge beneath the foundation reduces the rotation values as well as the damage level up to a desirable level.

The trenched inclined wall should have a greater shear strength compared with the surrounding soil. The wall should have the appropriate thickness (0.5 m for presented case) to allow some kind of flexible deflection and effectively reduce the damage level of the foundation. The studied cases showed that a mere 36° inclination is suitable enough to completely divert the rupture path.

The foundation position relative to the fault outcrop and the embedding of the foundation caused the mechanism of the fault rupture-foundation interaction to change. Based on the results obtained in this study, an inclined wall in combination with a trenched vertical wall is able to protect the foundation and reduce the sustained damage level to slight or moderate for most foundations at different positions.

There are two scenarios for the construction of concrete inclined wall: (1) for new buildings, the soil is excavated and the reinforced inclined wall is constructed and then soil is filled and compacted; and (2) for existing buildings, the desired stiffness of inclined wall is constructed by performing several rows of jet grout. However, the thickness and row's number of such jet grouting layer should be selected such that the *EI* is achieved. The use of an inclined jet grouting for ground treatment has been previously mentioned in some studies (Popa et al. 2001; Croce et al. 2014; Makowski and Polańska 2019; Pinto et al. 2003).

Data Availability Statement

All data generated or used during the study are available from the corresponding author per request.

References

ABAQUS. 2014. *ABAQUS analysis user's manual*. Providence, RI: Dassault Systèmes Simulia.

Abdoun, T., R. Dobry, T. D. O'Rourke, and S. H. Goh. 2003. "Pile response to lateral spreads: Centrifuge modelling." *J. Geotech. Geoenviron. Eng.* 129 (10): 869–878. https://doi.org/10.1061/(ASCE)1090-0241(2003)129:10(869).

Ahmed, W., and M. F. Bransby. 2009. "The interaction of shallow foundations with reverse faults." *J. Geotech. Geoenviron. Eng.* 135 (7): 914–924. https://doi.org/10.1061/(ASCE)GT.1943-5606.0000072.

Anastasopoulos, I., and G. Gazetas. 2007a. "Foundation–structure systems over a rupturing normal fault. Part I: Observations after the Kocaeli 1999 earthquake." *Bull. Earthquake Eng.* 5 (3): 253–275. https://doi.org/10.1007/s10518-007-9029-2.

Anastasopoulos, I., and G. Gazetas. 2007b. "Foundation–structure systems over a rupturing normal fault. Part II: Analysis of the Kocaeli case histories." *Bull. Earthquake Eng.* 5 (3): 277–301. https://doi.org/10.1007/s10518-007-9030-9.

Ashtiani, M., A. Ghalandarzadeh, M. Mahdavi, and M. Hedayati. 2018. "Centrifuge modeling of geotechnical mitigation measures for shallow foundations subjected to reverse faulting." *Can. Geotech. J.* 55 (8): 1130–1143. https://doi.org/10.1139/cgj-2017-0093.

Ashtiani, M., A. Ghalandarzadeh, and I. Towhata. 2016. "Centrifuge modeling of shallow embedded foundations subjected to reverse fault rupture." *Can. Geotech. J.* 53 (3): 505–519. https://doi.org/10.1139/cgj-2014-0444.

Azizkandi, A. S., S. Ghavami, M. H. Baziar, and S. H. Hasanaklou. 2019. "Assessment of damages in fault rupture–shallow foundation interaction due to the existence of underground structures." *Tunnelling Underground Space Technol.* 89 (Jul): 222–237. https://doi.org/10.1016/j.tust.2019.04.005.

Baziar, M. H., S. H. Hasanaklou, and A. S. Azizkandi. 2019. "Evaluation of EPS wall effectiveness to mitigate shallow foundation deformation induced by reverse faulting." *Bull. Earthquake Eng.* 17 (6): 3095–3117. https://doi.org/10.1007/s10518-019-00581-9.

Baziar, M. H., A. Nabizadeh, and M. Jabbari. 2014. "Numerical modeling of interaction between dip-slip fault and shallow foundation." *Bull. Earthquake Eng.* 13 (6): 1613–1632. https://doi.org/10.1007/s10518-014-9690-1.

Baziar, M. H., A. Nabizadeh, N. Khalafian, C. J. Lee, and W. Y. Hung. 2020. "Evaluation of reverse faulting effects on the mechanical response of tunnel lining using centrifuge tests and numerical analysis." *Géotechnique* 70 (6): 490–502. https://doi.org/10.1680/jgeot.18.P.019.

Bird, J. F., J. J. Bommer, H. Crowley, and R. Pinho. 2006. "Modeling liquefaction-induced building damage in earthquake loss estimation." *Soil Dyn. Earthquake Eng.* 26 (1): 15–30. https://doi.org/10.1016/j.soildyn.2005.10.002.

Bransby, M. F., M. C. R. Davies, A. El Nahas, and S. Nagaoka. 2008. "Centrifuge modelling of reverse fault–foundation interaction." *Bull. Earthquake Eng.* 6 (4): 607–628. https://doi.org/10.1007/s10518-008-9080-7.

Bray, J. D., A. Ashmawy, G. Mukhopadhyay, and E. M. Gath. 1993. "Use of geosynthetics to mitigation earthquake fault rupture propagation through compacted fill." In Vol. 1 of *Proc., Geosynthetics 93' Conf.*, 379–392. Roseville, MN: Industrial Fabrics Association International.

Choo, Y. W., D. S. Kim, K. H. Kim, D. H. Shin, E. S. Im, S. E. Cho, and H. G. Park. 2010. "Effect of drainage zoning and deeply placed plinth on CFGD." In Vol. 2 of *Proc., 7th Int. Conf. on Physical Modelling in Geotechnics*, 1177–1182. Boca Raton, FL: CRC Press.

Croce, P., A. Flora, and G. Modoni. 2014. *Jet grouting: Technology, design and control*. London: CRC Press.

Faccioli, E., I. Anastasopoulos, G. Gazetas, A. Callerio, and R. Paolucci. 2008. "Fault rupture—Foundation interaction: Selected case histories." *Bull. Earthquake Eng.* 6 (4): 557–583. https://doi.org/10.1007/s10518-008-9089-y.

Fadaee, M., I. Anastasopoulos, G. Gazetas, M. K. Jafari, and M. Kamalian. 2013. "Soil bentonite wall protects foundation from thrust faulting: Analyses and experiment." *Earthquake Eng. Eng. Vibr.* 12 (3): 473–486. https://doi.org/10.1007/s11803-013-0187-8.

Fadaee, M., P. Ezzatyazdi, I. Anastasopoulos, and G. Gazetas. 2016. "Mitigation of reverse faulting deformation using a soil bentonite wall: Dimensional analysis, parametric study, design implications." *Soil Dyn. Earthquake Eng.* 89 (Oct): 248–261. https://doi.org/10.1016/j.soildyn.2016.04.007.

Gazetas, G., A. Pecker, E. Faccioli, R. Paolucci, and I. Anastasopoulos. 2008. "Preliminary design recommendations for fault–foundation interaction." *Bull. Earthquake Eng.* 6 (4): 677–687. https://doi.org/10.1007/s10518-008-9082-5.

Hayward, T., A. Lees, W. Powrie, D. J. Richards, and J. Smethurst. 2000. *Centrifuge modelling of a cutting slope stabilized by discrete piles*. Rep. No. 471. Berkshire, UK: Transport Research Laboratory.

Kelson, K. I., K. H. Kang, W. D. Page, C. T. Lee, and L. S. Cluff. 2001. "Representative styles of deformation along the Chelungpu fault from the 1999 Chi-Chi (Taiwan) earthquake: Geomorphic characteristics and

responses of man-made structures." *Bull. Seismol. Soc. Am.* 91 (5): 930–952. https://doi.org/10.1785/0120000741.

Knappett, J. A., and S. P. G. Madabhushi. 2009. "Influence of axial load on lateral pile response in liquefiable soils. Part I: Physical modeling." *Géotechnique* 59 (7): 571–581. https://doi.org/10.1680/geot.8.009.3749.

Makowski, A., and B. Polańska. 2019. "Application of jet grouting technology for the renovation of historic buildings." In Vol. 1425 of *Proc., Journal of Physics: Conf. Series*. Bristol, UK: IOP Publishing. https://doi.org/10.1088/1742-6596/1425/1/012201.

Moghadam, A. M., A. Ghalandarzadeh, I. Towhata, M. Moradi, B. Ebrahimian, and P. Hajialikhani. 2009. "Studying the effects of deformable panels on seismic displacement of gravity quay walls." *Ocean Eng.* 36 (15–16): 1129–1148. https://doi.org/10.1016/j.oceaneng.2009.08.006.

Murbach, D., T. K. Rockwell, and J. D. Bray. 1999. "The relationship of foundation deformation to surface and near-surface faulting resulting from the 1992 Landers earthquake." *Earthquake Spectra* 15 (1): 121–144. https://doi.org/10.1193/1.1586032.

Oettle, N. K., and J. D. Bray. 2013. "Geotechnical mitigation strategies for earthquake surface fault rupture." *J. Geotech. Geoenviron. Eng.* 139 (11): 1864–1874. https://doi.org/10.1061/(ASCE)GT.1943-5606.0000933.

Pinto, A., J. Falcão, C. Barata, S. Ferreira, D. Cebola, and J. Pacheco. 2003. "Case histories of ground treatment with vertical jet grouting solutions." In *Proc., 3rd Int. Conf.: Grouting and Ground Treatment*, 401–412. Reston, VA: ASCE.

Popa, A., F. Lâcàtus, V. Rebeleanu, and O. Târlâ. 2001. "Underpinning of buildings by means of jet grouted piles." In *Proc., 15th Int. Conf. on Soil Mechanics and Geotechnical Engineering*, 1835–1838. Amsterdam, Netherlands: A.A. Balkema.

Puzrin, A. M., E. E. Alonso, and N. M. Pinyol. 2010. *Geomechanics of failures*. Dordrecht, Netherlands: Springer.

Ulusay, R., Ö. Aydan, and M. Hamada. 2002. "The behaviour of structures built on active fault zones: Examples from the recent earthquakes of Turkey." *J. Struct. Eng.* 19 (2): 149–167. https://doi.org/10.2208/jsceseee.19.149s.

White, D. J., W. A. Take, and M. D. Bolton. 2003. "Soil deformation measurement using particle image velocimetry (PIV) and photogrammetry." *Géotechnique* 53 (7): 619–631. https://doi.org/10.1680/geot.2003.53.7.619.

Zeping, X., H. Yujing, and L. Jianhui. 2014. "Three dimensional centrifuge modeling test of high CFRD in a narrow valley." In Vol. 2 of *Proc., 8th Int. Conf. on Physical Modelling in Geotechnics*, 899–902. Boca Raton, FL: CRC Press.